Raman spectroscopy of $SrRuO_3$ near the paramagnetic-to-ferromagnetic phase transition

M. N. Iliev, A. P. Litvinchuk, H.-G. Lee, C. L. Chen, M. L. Dezaneti, and C. W. Chu
Texas Center for Superconductivity, University of Houston, Houston, Texas 77204-5932

V. G. Ivanov, M. V. Abrashev, and V. N. Popov
Faculty of Physics, University of Sofia, BG 1126 Sofia, Bulgaria
(Received 21 May 1998; revised manuscript received 18 August 1998)

The polarized Raman spectra of (010)- and (001)-oriented epitaxial thin films of $SrRuO_3$ (space group $Pnma$, $Z=4$) are measured between 5 and 300 K. The Raman lines at 123, 225, 252, 291, 361, 390–393, and 412 cm^{-1} are assigned to definite modes of A_g or B_{2g} symmetry based of their polarization selection rules, the comparison with the results of lattice dynamical calculations (LDC), and accounting for the correlation between the Γ-point phonons in the $Pnma$ structure and the Γ-, R-, X-, and M-point phonon modes in the parent $Pm\bar{3}m$ structure. The pronounced anomalies of the Raman phonon parameters near the ferromagnetic transition ($T_c=148$ K) are discussed in terms of enhanced spin-phonon coupling and reorganization of the electronic states in the vicinity of T_c. [S0163-1829(99)12301-4]

I. INTRODUCTION

$SrRuO_3$ crystallizes in the perovskitelike orthorhombic $Pnma$ structure.[1] It attracts significant interest as it has a metallic behavior, exhibits a ferromagnetic ordering below $T_c \approx 150$ K, and can be grown epitaxially on different oxide substrates, including high temperature superconductors.[2–4] Kirillov *et al.*[5] reported the nonpolarized Raman spectra from (101)-oriented $SrRuO_3$ thin films. Six Raman lines have been observed in that study. However, no assignment of those lines to particular phonon modes has been attempted.[6]

In this work we report the polarized Raman spectra of epitaxially grown (010)- and (001)-oriented $SrRuO_3$ thin films. On the basis of their polarization selection rules and by comparison with the results of lattice dynamical calculations we assigned the observed Raman lines to definite modes of A_g and B_{2g} symmetry. We also observed and studied in more detail the anomalies near the ferromagnetic transition temperature of some phonon parameters, which have partly been discussed earlier.[5]

II. SAMPLES AND EXPERIMENTAL

The (010)- and (001)-thin films used in our study were ≈ 3000 Å thick and were grown epitaxially by pulsed laser deposition on (100)- and (110)-oriented $SrTiO_3$ substrates, respectively. Details of their growth and characterization are given elsewhere.[3,4] The cross-sectional HREM and TEM images gave no indications for strained areas close to the $SrRuO_3/SrTiO_3$ boundary. It is worth noting that for strongly light absorbing materials like $SrRuO_3$ the scattering volume is restricted to 1000–2000 Å below the sample surface thus not including the $SrRuO_3/SrTiO_3$ boundary region where strains may affect the lattice. The Raman spectra were measured using a S3000 (Jobin-Yvon) triple spectrometer equipped with a microscope and a liquid-nitrogen-cooled CCD detector. The samples were mounted in a Microstat^{He} cryostat (Oxford Instruments) where the temperature could be varied between 5 and 300 K. The spectra were measured in backward scattering configuration using the 514.5 nm laser line of an Ar^+ laser. An objective of $\times 50$ magnification was used to both, focus the laser beam in a spot of ~ 5 μm diameter on the sample's surface, and collect the scattered light. As the crystallographic directions [100] and [001] [for the (010)-oriented film], as well as the [100] and [010] [for the (001)-oriented film], were well defined, we were able to perform measurements in several exact scattering configurations, namely $xx(zz)$, yy, $x'x'(z'z')$, $xz(zx)$, and $yx(yz)$. In these notations x, y, and z are along the directions of a, b, and c, respectively, whereas x' and z' are two orthogonal directions in the xz-plane, rotated by 45 degrees with respect to the x and z axes. The x and z directions are not distinguishable because of very close a and c parameters and possible twinning.

III. Γ-POINT PHONON MODE ANALYSIS

Table I summarizes the results of group-theoretical analysis for the Γ-point phonon modes of $SrRuO_3$ (space group $Pnma$, $Z=4$). Of the total 60 Γ-point phonons, $24(7A_g+5B_{1g}+7B_{2g}+5B_{3g})$ are Raman-active, $25(9B_{1u}+7B_{2u}+9B_{3u})$ are infrared-active, $8(8A_u)$ are silent, and $3(B_{1u}+B_{2u}+B_{3u})$ are acoustic phonons. The Raman lines of a given symmetry have to be observed in the corresponding allowed scattering configurations. As to the assignment of a particular Raman line to definite atomic motions, it could be based on a comparison with the results of lattice dynamical calculations, as well as on some additional arguments concerning the compatibility relations between the symmetries of the Γ_o-point phonons of the orthorhombic $Pnma$ structure and those of the R_c, M_c, and X_c zone-boundary phonons of the cubic $Pm\bar{3}m$ structure. Indeed, the orthorhombic structure of $SrRuO_3$ results from a distortion of the ideal cubic perovskite structure. Both structures are compared in Fig. 1, where the corresponding reciprocal cells (first Brillouin zones) are also shown. The orthorhombic reciprocal cell is four times smaller than the cubic one, and the

TABLE I. Wyckoff notations, atomic site symmetries, fractional atomic coordinates and the irreducible representations for the atoms in orthorhombic $SrRuO_3$ (the atomic positions at 100 K are from Ref. 7).

Atom	Wyckoff notation	Site symmetry	x	y	z	Irreducible representations
Sr	4(c)	C_s	0.0196	0.2500	−0.0025	$2A_g+B_{1g}+2B_{2g}+B_{3g}+A_u+2B_{1u}+B_{2u}+2B_{3u}$
Ru	4(b)	C_i	0.0000	0.0000	0.5000	$3A_u+3B_{1u}+3B_{2u}+3B_{3u}$
O1	4(c)	C_s	0.5000	0.2500	0.550	$2A_g+B_{1g}+2B_{2g}+B_{3g}+A_u+2B_{1u}+B_{2u}+2B_{3u}$
O2	8(d)	C_1	0.2774	0.0283	0.7226	$3A_g+3B_{1g}+3B_{2g}+3B_{3g}+3A_u+3B_{1u}+3B_{2u}+3B_{3u}$

Modes classification

$\Gamma_{\text{Raman}}=7A_g+5B_{1g}+7B_{2g}+5B_{3g}$
$A_g\rightarrow\alpha_{xx},\alpha_{yy},\alpha_{zz}$
$B_{1g}\rightarrow\alpha_{xy},\alpha_{yx}$
$B_{2g}\rightarrow\alpha_{xz},\alpha_{zx}$
$B_{3g}\rightarrow\alpha_{yz},\alpha_{zy}$

$\Gamma_{\text{ir}}=9B_{1u}+7B_{2u}+9B_{3u}$
$\Gamma_{\text{silent}}=8A_u$
$\Gamma_{\text{acoustic}}=B_{1u}+B_{2u}+B_{3u}$

Γ_o-point phonon modes of the orthorhombic Brillouin zone are related to either Γ_c zone-center or R_c, M_c, and X_c zone-boundary modes of the cubic Brillouin zone.[8] In particular, the Raman-active modes of the orthorhombic structure originate from the R_c, M_c, and X_c phonon modes of the cubic $Pm\bar{3}m$ structure, the correspondence being as follows:

$$7A_g\rightarrow R'_{15}+2R'_{25}+2X_5+M_2+M_3$$

$$5B_{1g}\rightarrow R_{12}+R'_{15}+2X_1+M_5$$

$$7B_{2g}\rightarrow R'_{15}+2R'_{25}+2X_5+M_1+M_4$$

$$5B_{3g}\rightarrow R_1+R_{12}+2R'_{25}+M_5.$$

As the atomic displacements and, hence, the distortions of the cubic symmetry in the case of $SrRuO_3$ are relatively small, it is plausible to expect that the Raman modes of different symmetry originating from the same otherwise degenerate zone-boundary cubic phonon mode $[R_{12}(2), R'_{15}(3), 2R'_{25}(3), 2X_5(2)$, and $M_5(2)]$ will have close wave numbers.

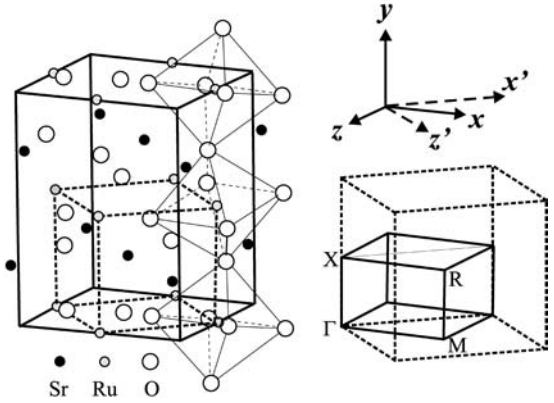

FIG. 1. Unit-cell and first Brillouin zone of $SrRuO_3$ (space group $Pnma$). The unit cell and the first Brillouin zone of the simple perovskite structure (space group $Pm\bar{3}m$) are also shown with dashed lines.

IV. LATTICE DYNAMICAL CALCULATIONS

The assignment of the observed Raman modes was supported by shell model calculations of the lattice dynamics of $SrRuO_3$. This model gives an adequate picture of the vibrations in perovskitelike structures because it accounts for their predominant ionicity. The ionic interactions are represented by long-range Coulomb potentials and short-range repulsive potentials of the Born-Mayer form. The deformation of the electron charge density of the ions is described in the dipole approximation considering each atom as consisting of a point charged core and a concentric spherical massless shell with charge Y. Each core and its shell are coupled together with a force constant k giving rise to the free ionic polarizability α given by

$$\alpha=\frac{Y^2}{k}. \tag{1}$$

The model parameters for the strontium and oxygen ions and their interaction potential are taken from previous studies of simpler compounds with perovskitelike structure.[9] For the ruthenium ions and their interaction potential with the oxygen ions, the parameters for titanium obtained from titanates were adopted[10] because of the same ionic charges and similar ionic radii. Due to this, a few of the calculated frequencies show disagreement up to 10 percent with the corresponding measured ones of A_g and B_{2g} symmetry. As a whole, the model results reproduce well the observed Raman-active phonons and it can be concluded that they predict well the unobserved optical phonons.

V. RESULTS AND DISCUSSION

A. Phonon mode assignment

Figure 2 shows the Raman spectra of $SrRuO_3$ as measured at a nominal temperature of 5 K. In the $z(yy)\bar{z}$ spectrum

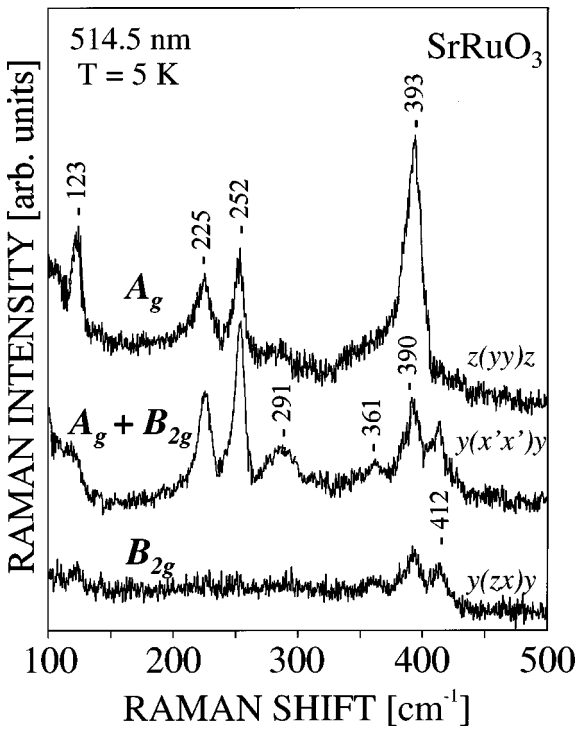

FIG. 2. Raman spectra of $SrRuO_3$ as obtained at 5 K with three exact scattering configurations.

where only the Raman modes of A_g symmetry have to be pronounced, one observes Raman lines at 123, 225, 252, and 393 cm^{-1}. In the $z(xx)\bar{z}$ spectrum (not shown here) where also only the A_g lines are allowed and in the $y(x'x')\bar{y}$ spectrum (A_g+B_{2g}) the 123 cm^{-1} line is of negligible intensity whereas a new weak line is observed near 291 cm^{-1}. No detectable Raman lines were present with the crossed $z(xy)\bar{z}$ and $z(yx)\bar{z}$ scattering configurations which is an indication that the B_{1g} (or B_{3g}) lines are of negligible intensity. Given the directions of $a(x)$ and $c(z)$ on the surface of the (010)-oriented thin film were known, we could measure the Raman spectra in the following exact scattering configurations: $y(xx)\bar{y}$ (A_g), $y(xz)\bar{y}$ (B_{2g}), and $y(x'x')\bar{y}$ (A_g+B_{2g}). As follows from their appearance in the cross-polarized $y(xz)\bar{y}$ configuration, there are two relatively strong (at 390 and 412 cm^{-1}) and one weaker (at 361 cm^{-1}) Raman modes of B_{2g} symmetry. The 412 cm^{-1} line can still be observed in the $y(xx)\bar{y}$ spectrum [compare to the $z(xx)\bar{z}$ spectrum], which could be explained by a slight misorientation of a and c axes with respect to light polarization directions.

In Fig. 3 are shown the main atomic motions and the wave numbers (in brackets) for the A_g and B_{2g} modes of $SrRuO_3$, as obtained from the lattice dynamical calculations. A tentative assignment of the experimentally observed Raman lines to definite modes is also given. While for the low-

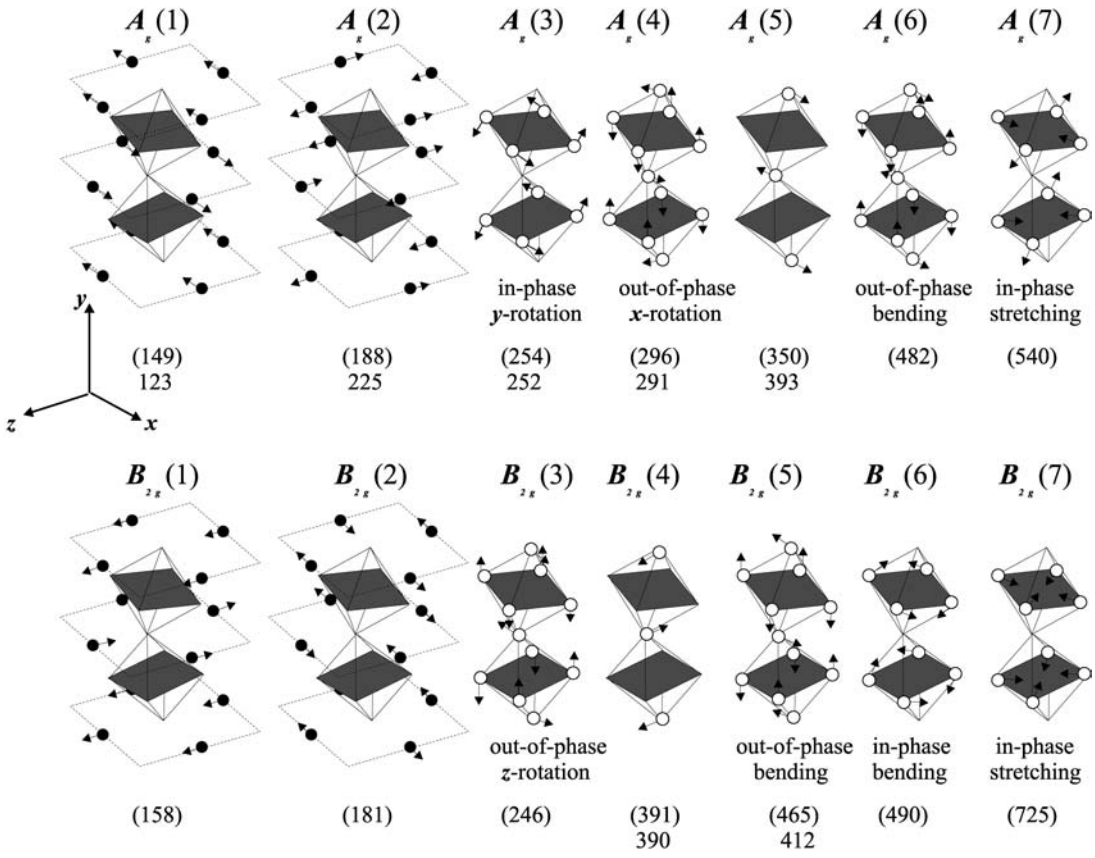

FIG. 3. The main atomic motions and the wave numbers (in brackets) for the A_g and B_{2g} modes of $SrRuO_3$, as obtained from the lattice dynamical calculations. A tentative assignment of the experimentally observed Raman lines to definite modes is also given.

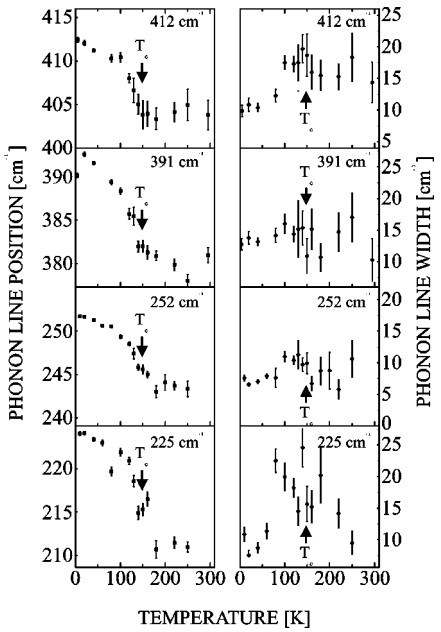

FIG. 4. Temperature dependence of the position and linewidth of four of the Raman lines of $SrRuO_3$.

frequency Sr modes there is a relatively large discrepancy between the calculated and experimental values, the oxygen modes are satisfactorily described by the shell model. In particular, the appearance of the Raman lines of different symmetry at close wave numbers [A_g at 393 cm^{-1} and B_{2g} at 390 cm^{-1}] finds explanation in their origin from the same degenerated zone-boundary phonon (in this case the X_5-point phonon) in the parent $Pm\bar{3}m$ structure.

B. Phonon anomalies near the ferromagnetic transition

As it is already mentioned, $SrRuO_3$ undergoes upon cooling the transition from paramagnetic to spin ordered ferromagnetic state at $T_c \approx 148$ K. Ru sublattice magnetization does influence the dynamic properties of the lattice, as it was shown by Kirillov *et al.*[5] In order to study the effects in more detail we performed Raman measurements on the (010) thin film in the temperature range 5–300 K, which covers the transition temperature T_c. The results are summarized in Fig. 4, where the temperature dependence of the frequency and linewidth for selected phonons are displayed.

In the discussion let us first note that the magnetic ordering transition in $SrRuO_3$ is not accompanied by a structural transition, as it is the case of, e.g., cupric oxide CuO.[11] This latter material exhibits new Raman-active lines upon entering the magnetically ordered state, which are due to an increase of the unit cell volume. In $SrRuO_3$, however, no additional lines appear upon cooling below T_c. Nevertheless, one clearly observes change of the phonon parameter variation at temperatures where magnetic ordering occurs. Generally speaking, one could expect such changes for phonons, which involve ion motions that modulate spin exchange coupling (see Ref. 11 and references cited therein). In the case of $SrRuO_3$ representative phonons of this type are ''apical'' oxygen vibrations $A_g(5)$ and $B_{2g}(4)$ in Fig. 3, which modulate the Ru-O-Ru bond angle (Ru ions are situated at the centers of shaded squares). These vibrations are predicted to occur at 350 cm^{-1} and 391 cm^{-1} and found experimentally at 391 and 393 cm^{-1}, respectively. As it is seen from Fig. 4, however, other Raman lines including the one near 225 cm^{-1} (assigned to a mode involving mainly Sr motions) also show a remarkable change of the frequency vs temperature dependence around T_c. This is an indication for either more complex mechanism of spin-phonon coupling or strong mixing of phonon modes.

Although the phonon linewidths were extracted with a relatively large error, one can trace a well defined maximum around T_c, unlike the steplike behavior observed by Kirillov *et al.*[5] for the mode they have observed at 94 cm^{-1} (our frequency range was restricted down to 100 cm^{-1} and we cannot directly compare the results for this particular mode). This maximum is a signature for a coupling between the optical phonons and the long-range fluctuations of the order parameter which is known to diverge in the vicinity of the second order phase transition.

An important question which arises concerns the mechanism of the phonon-spin coupling. As already mentioned, the exchange interaction between two Ru ions is sensitive to the Ru-O bond lengths and interbond angles. For this reason frequency of oxygen phonon modes are expected to be affected by Ru spins alignment below T_c. Recent results by Kim *et al.*[12] show that it is indeed a fact for infrared active vibrations of perovskitelike $La_{0.7}Ca_{0.3}MnO_3$. It was firmly established that lattice contraction upon cooling is not solely responsible for the large (up to 20 cm^{-1}) observed phonon hardening below T_c because it would require unrealistic dependence of the mode frequency vs interatomic spacing $\omega_{ph} \propto a^{-20}$. Alternatively, Kim *et al.* proposed that the IR-phonon hardening stems from a decrease of the free carrier (assumed to be large polarons) screening due to a broadening of the conduction zone.[12]

To our knowledge, no data on temperature variation of the lattice parameters around T_c are available for $SrRuO_3$. However, due to the similarly large phonon hardening compared to the case of $La_{0.7}Ca_{0.3}MnO_3$, we assume that the decrease of the lattice parameters upon cooling can only partially explain the observed frequency shift in $SrRuO_3$ and that a significant reorganization of the electronic states occurs in the vicinity of T_c similarly to the doped lanthanum manganate. As mentioned above, the observed temperature anomalies are a rather general phenomenon for all the optical phonons in the structure, irrespectively on the bond lengths and bond angles being modulated. Thus, it is reasonable to relate the changes in the lattice dynamics to the reorganization of the electronic band structure which takes place around the phase transition and more precisely, to the variations of the density of the itinerant carriers.

To make at least qualitative conclusions we take the simplest possible approach based on the electron-gas model which is in fact the Thomas-Fermi approximation for the total energy of the crystal. It takes the advantage of using only the local electronic density independently on the exact nature of the involved electronic states, localized or extended. For this reason the electronic-gas models has been developed and widely applied to the calculation of forces between free, closed-shell atoms and ions[14] as well as the stability and the lattice dynamics of insulating ionic crystals where no electronic transport takes place.[15,16] Therefore, we

believe that the model predictions will not confront with the recent findings of Klein *et al.*[13] which reveal a strongly correlated, almost localized electronic transport in $SrRuO_3$.

It is plausible to assume that the free carriers contribute to the effective force constants for the Raman-active modes through $1/\kappa$ with κ being the compressibility of the electronic gas. In the simplest Fermi-gas picture one has

$$\frac{1}{\kappa} \propto \frac{\hbar^2 n^{5/3}}{m^*}, \tag{2}$$

where n and m^* are the concentration and the effective mass of free charge carriers, respectively. A recent optical reflectivity study of $SrRuO_3$ shows that the plasma frequency, which is determined by the ratio n/m^*, is independent on the temperature in broad temperature range despite of an increase of the effective mass upon cooling.[17] This is due to a similar change with temperature of the concentration of the carriers and their effective mass. However, one expects an increase of the effective force constant because, according to Eq. (2), it depends superlinearly on n which increases upon cooling. Thus the pronounced phonon hardening below T_c in $SrRuO_3$ is determined not only by the anharmonicity-related effects, but to a great extend also by an increase of the free charge carriers concentration upon cooling due to the delocalization of some electronic (or polaronic) states.

VI. CONCLUSION

By means of Raman scattering we have studied polarized scattering spectra of oriented $SrRuO_3$ films over the temperature range 5–300 K. The observed phonon modes are assigned to the definite modes of A_g and B_{2g} symmetry based on their polarization properties and comparison with the results of the shell model lattice dynamic calculations. Phonon frequencies and linewidths are found to be strongly affected by the transition of $SrRuO_3$ from high temperature paramagnetic to spin ordered ferromagnetic state at $T_c \approx 148$ K: the linewidth exhibit a maximum around T_c and frequency shows pronounced hardening upon cooling below the spin ordering temperature, which is an evidence for strong electron-phonon coupling in $SrRuO_3$.

ACKNOWLEDGMENTS

This work was supported by the ARPA MDA-90-J-1001, the State of Texas through the Texas Center for Superconductivity at the University of Houston (TCSUH), and the NSF through the Material Research Science and Engineering Center at the University of Houston (MRSEC-UH).

[1] C. B. Eom, R. J. Cava, R. M. Fleming, Julia M. Phillips, R. B. van Dover, J. H. Marshall, J. W. P. Hsu, J. J. Krajewski, and W. F. Peck, Jr., Science **258**, 1766 (1992).

[2] L. Antognazza, K. Char, T. H. Geballe, L. L. H. King, and A. W. Seight, Appl. Phys. Lett. **63**, 1005 (1993).

[3] C. L. Chen, Y. Cao, Z. J. Huang, Q. D. Jiang, Z. H. Zhang, Y. Y. Sun, W. N. Kang, L. M. Dezaneti, W. K. Chu, and C. W. Chu, Appl. Phys. Lett. **71**, 1047 (1997).

[4] C. L. Chen, Y. Cao, Z. J. Huang, Z. H. Zhang, A. Brazdeikis, Q. D. Jiang, I. A. Rusakova, Y. Y. Sun, W. K. Chu, and C. W. Chu (unpublished).

[5] D. Kirillov, Y. Suzuki, L. Antognazza, K. Char, I. Bozovic, and T. H. Geballe, Phys. Rev. B **51**, 12 825 (1995).

[6] The classification of the Raman-active modes of $SrRuO_3$ given in Ref. 5 ($5A_g+4B_{1g}+4B_{2g}+4B_{3g}$) is incorrect. Instead, as follows from Table I, $7A_g+5B_{1g}+7B_{2g}+5B_{3g}$ Raman modes are allowed.

[7] J. S. Gardner, G. Balakrishnan, and D. McK. Paul, Physica C **252**, 303 (1995).

[8] Ph. Daniel, M. Rousseau, A. Desert, A. Ratuszna, and F. Ganot, Phys. Rev. B **51**, 12 337 (1995).

[9] V. Popov, J. Phys.: Condens. Matter **7**, 1625 (1995).

[10] M. V. Abrashev, C. Thomsen, V. N. Popov, and L. N. Bozukov, Physica C **274**, 141 (1997).

[11] X. K. Chen, J. C. Irwin, and J. P. Franck, Phys. Rev. B **52**, R13 130 (1995).

[12] K. H. Kim, J. Y. Gu, H. S. Choi, G. W. Park, and T. W. Noh, Phys. Rev. Lett. **77**, 1877 (1996).

[13] L. Klein, J. S. Dodge, C. H. Ahn, G. J. Snyder, T. H. Geballe, M. R. Beasley, and A. Kapitulnik, Phys. Rev. Lett. **77**, 2774 (1996).

[14] R. G. Gordon and Y. S. Kim, J. Chem. Phys. **56**, 3122 (1972).

[15] C. Muhlhausen and R. G. Gordon, Phys. Rev. B **23**, 900 (1981).

[16] R. E. Cohen, L. L. Boyer, and M. J. Mehl, Phys. Rev. B **35**, 5749 (1987).

[17] P. Kostic, Y. Okada, N. C. Collins, Z. Schlesinger, J. W. Reiner, L. Klein, A. Kapitulnic, T. H. Geballe, and M. R. Beasley, Phys. Rev. Lett. **81**, 2498 (1998).